CHEMIJA. 2022. Vol. 33. No. 3. P. 65–72
© Lietuvos mokslų akademija, 2022

Corrosion resistance of AZ31 alloy after treatment with high current density impulse or/and laser irradiation in Hank's solution

Gedvidas Bikulčius,

Svetlana Lichušina*,

Vidas Pakštas,

Mindaugas Gedvilas,

Voitech Stankevič,

Aušra Selskienė,

Asta Grigucevičienė

Center for Physical Sciences and Technology (FTMC), 3 Saulėtekio Avenue, 10257 Vilnius, Lithuania

In this article, we have introduced a new method that can improve the corrosion resistance of AZ31 alloy. We compared the biodegradation of AZ31 alloy foil treated with a high current density impulse (HCDI), laser irradiation (LI) and HCDI-LI with that of the untreated one. The rate of the biodegradation of AZ31 alloy treated with HCDI-LI was lower than those of the untreated one, the alloy treated with HCDI or LI. Thus, the improved corrosion resistance of the AZ31 alloy treated with HCDI-LI allows its use for medical purposes.

Keywords: magnesium alloys, high current density impulse (HCDI), laser irradiation (LI), corrosion

INTRODUCTION

Magnesium alloys are the most promising materials for biomedical application as temporary bioresorbable implants, which do not require the process of implant removal [1, 2]. The high corrosion rate of Mg alloys has hindered their wider use in orthopedic applications. The high current density impulse (HCDI) method [3–5] or laser irradiation (LI) surface treatment can be used to reduce the corrosion rate of magnesium alloys [6–8].

The treatment of metals and alloys by using the HCDI method can change their structure, dislocation movements and oriented microstructure [3]. Obviously, this will affect the mechanical properties of the material and the rate of corrosion. Babutsky et al. [4–5] showed that the use of pulsed current density up to 3.0 kA/mm^2 for aluminum 5182 and 5754 alloys only slightly increases the corrosion resistance.

The laser shock peening (LSP) method makes it possible to change the surface microstructure and residual stresses of metals and their alloys [6]. For example, the LSP treatment of AZ31B alloy changes the residual surface stress from tensile to compression, and the latter already contributes to increase in the corrosion resistance of magnesium. Ge et al. [7] found that the LSP treatment of AZ31B alloy not only alters residual stress, but also forms a refined grain structure. This has a positive effect on the corrosion resistance of AZ31B alloy in a simulated body fluid. Jana et al. [8] showed that the treatment of AZ31 alloy surface with laser irradiation (LI) increased its corrosion resistance by about 3 times in a 5 wt.% NaCl solution. In addition, its localised corrosion is more pronounced without laser treatment, compared with that after laser treatment.

* Corresponding author. Email: svetlana.lichusina@ftmc.lt

The study aims at investigation of the corrosion resistance of AZ31 alloy after the high current density impulse and/or laser irradiation treatment of AZ31 alloy to improve its application in biomedicine.

EXPERIMENTAL

Commercial AZ31 foil (Mg-2.46Al-0.81Zn, wt.%) was used as a substrate. The surface of AZ31 foil with dimensions of 21 mm × 21 mm × 0.25 mm (Sigma-Aldrich) was pre-cleaned, applying 2500 grit paper. After polishing and wiping with acetone (HPLC Plus grade, Sigma-Aldrich), specimens were subjected to ultrasonication for 10–15 min in isopropanol and drying under nitrogen flow. A pulsed current generator consisting of a power supply with a capacitor (5.2 mF) and an integrated oscilloscope (Tektronix DPO 3052) was used for the HCDI treatment of AZ31 alloy. As shown in the previous potentiodynamic studies of AZ31 foil in Hank's solution, the optimal high current density pulse (HCDI) mode is 1800 A/mm^2 at 0.5 ms. A nanosecond laser (Baltic HP, Ekspla) working at a fundamental wavelength of 1064 nm, a pulse duration of 10 ns, a pulse energy of 60 μJ, a pulse repetition rate of 10 kHz and an average optical power of 6.0 W were used in bidirectional hatch patterning. The setup of the experiment is shown in Fig. 1a. The scanning of a laser beam on the sample surface was performed with a galvo scanner (Scangine 14, Scanlab). The Gaussian beam spot radius on the sample was w_0 = 23 μm (1/e^2 level). Laser beams scanning in spiral trajectory on the sample surface at a constant speed of 460 mm/s caused an overlapping laser beam spot (Fig. 1b). The pulse overlap distance was Δx = 46 μm. The hatch distance between two advanced lines in bidirectional trajectory was Δy = 23 μm. The Gaussian beam laser fluence in the center of the beam was F_0 = 7.2 J/cm^2. The Gaussian beam overlap in y direction was 50% at $\Delta y = w_0$. XRD patterns of AZ31 samples were measured using an X-ray diffractometer SmartLab (Rigaku) equipped with a 9 kW rotating Cu anode X-ray tube. The grazing incidence (GIXRD) method was used in the 2θ range 15–75°. The angle between the parallel beam of X-rays and the specimen surface (ω angle) was adjusted to 0.5°. Phase identification was performed using the software package PDXL-2 (Rigaku) and ICDD powder diffraction data-base PDF-4+ (2021 release). The crystallite size was calculated using

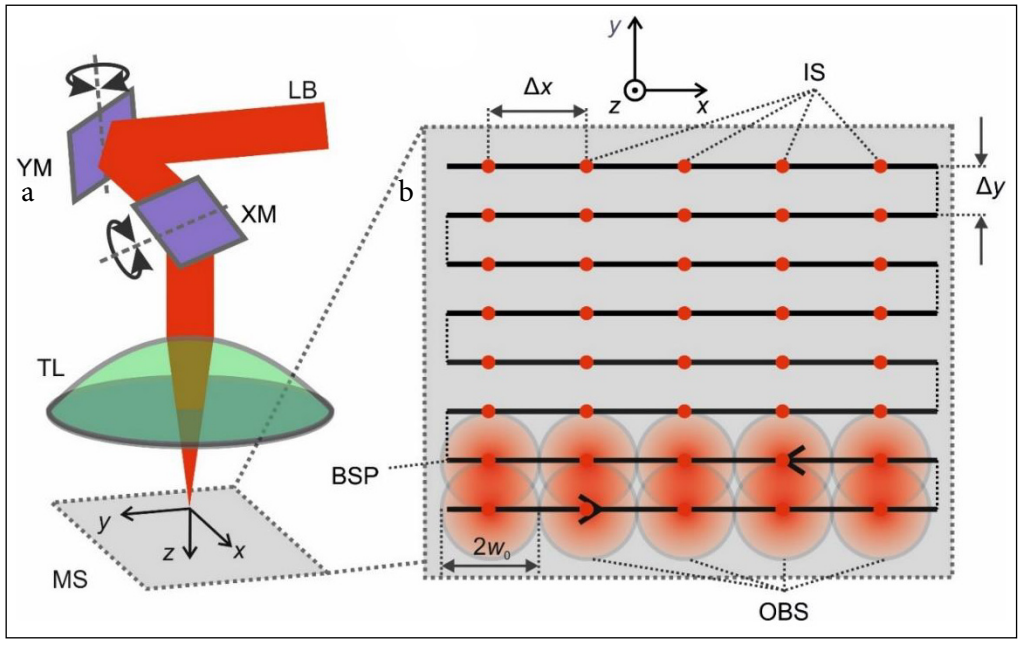

Fig. 1. Experiment setup and a bidirectional laser beam scanning procedure. (a) Principal scheme of the laser patterning experiment with a focused beam: LB, laser beam; XM and YM, *x*- and *y*-mirrors controlled by galvanometric motors; TL, telecentric *f*-theta lens; MS, magnesium sample; *xyz*, coordinate system. (b) Schematic representation of a bidirectional scan pattern (BSP) with an indicated scanning direction by black arrows, and overlapping beam spots (OBS) with red dots indicating irradiation spots (IS), $2w_0$ is the laser spot diameter on the sample, Δx is the pulse overlap distance and Δy is the hatch distance

the graphical Halder–Wagner method implemented in the PDXL software package (Rigaku). The approach is based on the graphical representation of the linear relationship $(\beta/\tan\theta)^2$ vs $\beta/(\tan\theta \sin\theta)$ plot (where β is the XRD peak physical broadening and θ is the diffraction angle).

An optical microscope and dual-beam system Helios Nanolab 650 (SEM) equipped with an energy-dispersive X-ray spectrometer (EDX) (Oxford Instruments, X max 20 mm^2 detector, INCA 4.15 software) were used for the investigation of sample surface. The corrosion characteristics were determined by open circuit potential monitoring (OCP) and the potentiodynamic polarisation (PDP) technique using a P/G/FRAsystem Solartron 1280C (Ametek, Inc.). All the tests were performed at a temperature of 37°C in a naturally aerated Hank's balanced salt solution (HBSS) from Sigma-Aldrich Chemie GmbH, whose composition was as follows (g L^{-1}): $0.185CaCl_2 \times 2H_20$, $0.097MgSO_4$, $0.4KCl$, $0.06KH_2PO_4$, 0.35 $NaHCO_3$, 8.0 NaCl, 0.048 Na_2HPO_4, 1.0 glucose and 0.011 Phenol Red, pH 7.2–7.6. An Ag/AgCl electrode in a saturated KCl solution was used as reference and the potentials all through the paper were referred to this electrode. The tested surface area of the working electrode was 0.5 cm^2. The Tafel polarisation curves were measured in the potentiodynamic mode at a potential scan rate of 1 mV s^{-1}.

The immersion corrosion tests of AZ31 alloy in Hank's solution were performed using a glass tube with 60 ml volume pressed through a rubber gasket to the 2.83 cm^2 surface of the sample exposed to the solution. All immersion containers were kept at 37.5 ± 0.5°C in the furnace for up to 72 h. Samples were weighed before and after the exposure. The ratio of the solution volume to the specimen area was 20 mL cm^{-2} according to the ASTM G31-72 standard. The immersion solution was refreshed every 3 days. The samples were removed from the solution at a certain time, gently rinsed with distilled water and dried in air for observation. The corrosion products were removed in chromic acid solution (180 g/l) at room temperature for 30 min, then washed with ethanol and finally dried in air.

RESULTS AND DISCUSSION

The XRD profiles of the untreated AZ31 alloy, and the ones treated with HCDI, LI and HCDI-LI are shown in Fig. 2a–c. The obtained diffraction peaks are rather broad, which indicates that the Mg-Al

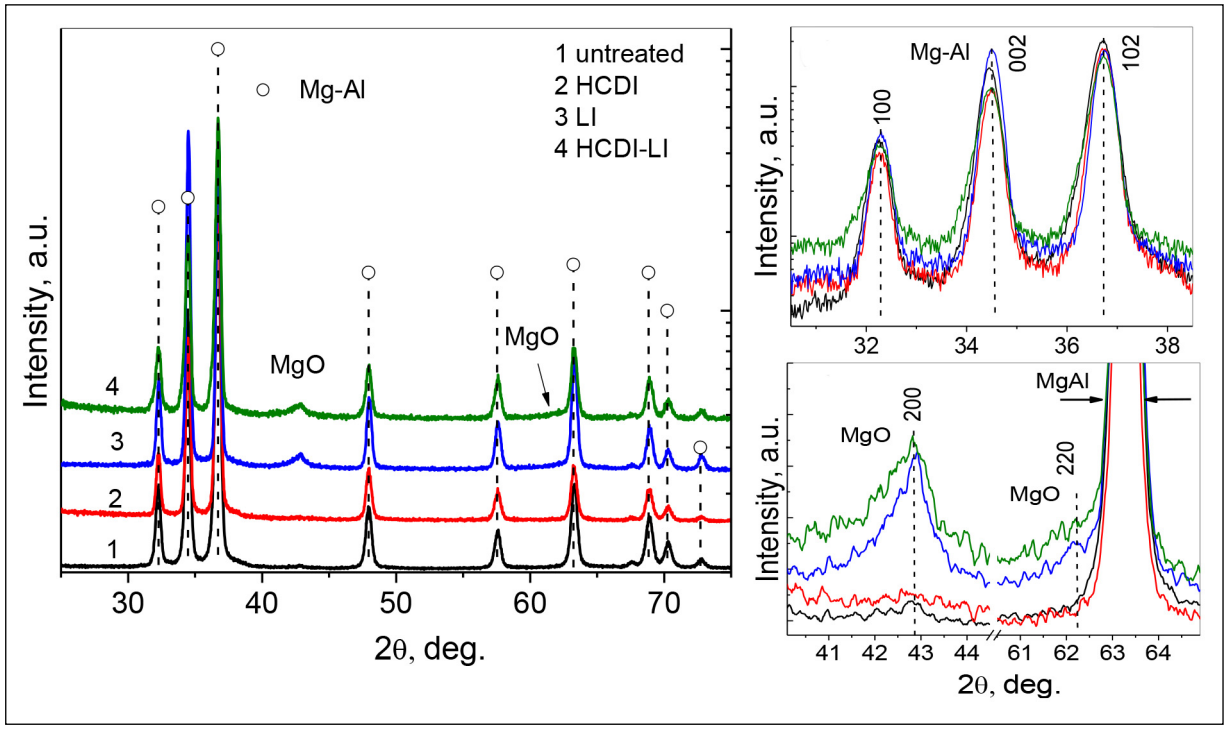

Fig. 2. XRD patterns of AZ31 alloy depending on the treatment method. (a) Survey spectra, (b) a zoomed-in view of Mg-Al peaks and (c) a zoomed-in view of MgO peaks

phase (ICDD#04-003-5035) is composed of small crystallites with an average size of 20.6 ± 0.3 nm. After the LI treatment, the Mg-Al crystallites increase up to 23.8 ± 0.5 nm, the HCDI treatment practically does not affect the size of the crystallites. Meanwhile, after the HCDI-LI treatment of AZ31 alloy, the size of Mg-Al phase crystallites decreased to 16.2 ± 0.3 nm. After the AZ31 alloy treatment with HCDI, LI and HCDI-LI, the Mg-Al diffraction peaks maintain their positions, indicating that the phase composition of the alloy does not change (Fig. 2b). This means that the structure of AZ31 alloy does not change and no solid solution of the changed chemical composition is formed. An increase in the intensity of the cubic structure MgO (ICDD # 00-004-0829) peaks at 2 theta = 42.91 and 62.31 ° (200 and 220) as compared to that of the untreated alloy sample was observed for the laser-treated samples. The integral area of the MgO peaks at peak (200) is quite similar (LI treatment 490 and HCDI-LI 522 cps. deg., respectively), indicating that the HCDH treatment does not significantly affect MgO formation, as opposed to the laser treatment. The resulting MgO diffraction peaks are quite broad, indicating that the MgO phase consists of small crystallites (Fig. 2c).

The optical images of AZ31 alloy after the potentiodynamic investigation are shown in Fig. 3. These pictures show black traces of local corrosion (Fig. 3a–d). In the case of untreated AZ31 alloy, the local corrosion foci are grouped along the perimeter resembling crack corrosion (Fig. 3a). Meanwhile, in the case of HCDI treatment the local corrosion sites were more evenly distributed on the surface of AZ31 alloy (Fig. 3b). The surface treatment of AZ31 alloy with laser irradiation (LI) changes the type of localised corrosion. It resembles evenly distributed pitting corrosion. The local corrosion of HCDI-LI treated samples is similar to that of only laser irradiated ones (Fig. 3c).

Figure 4a shows the open circuit potential of the untreated AZ31, HCDI and LI, and HCDI-LI treated samples in the Hank's solution for 3600 s. The OCP curves of untreated and HCDI treated AZ31 samples during the first 100 s rapidly increase to a maximum and reach a stable potential, followed by potential fluctuations. The OCP curves of LI and HCDI-LI treated samples gradually increase and do not reach a stable potential. The OCP after 3600 s for untreated, HCDI and LI, and HCDI-LI treated samples are –1.50, –1.50, –1.48, and –1.57 V, respectively.

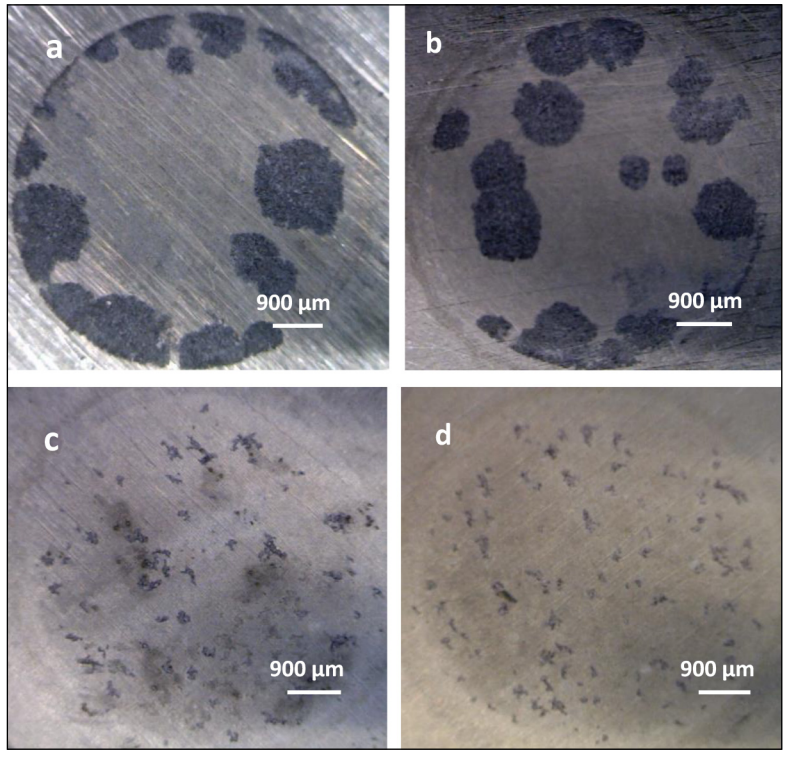

Fig. 3. Optical images of AZ31 alloy after potentiodynamic tests in Hank's solution: (a) untreated and treated (b) with HCDI, (c) with LI, (d) with HCDI-LI

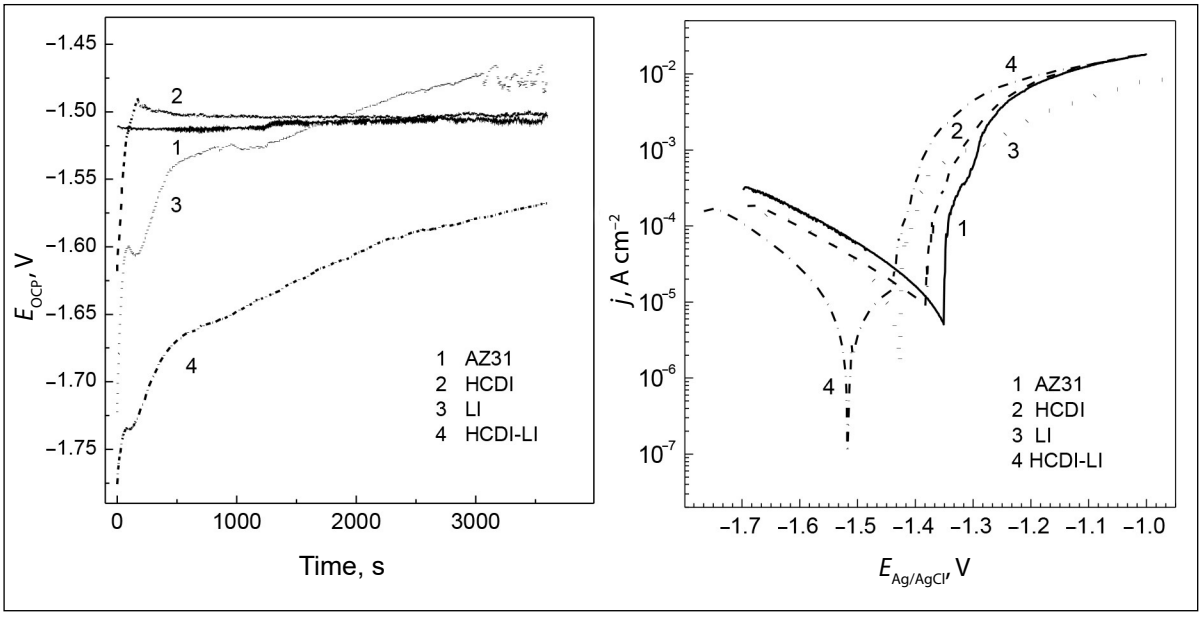

Fig. 4. Evolution of the open circuit potential (a) and potentiodynamic curves (b) for AZ31 foil obtained in Hank's solution: (1) untreated and treated (2) with HCDI, (3) with LI, (4) with HCDI-LI

Three groups of characteristic parameters, such as the corrosion potential (E_{corr}), corrosion current density (i_{corr}) and cathodic Tafel slope (βc) were obtained by fitting the polarisation curves (Fig. 4b). These data are listed in Table 1. Notably, the HCDI treated samples showed the highest corrosion potential (–1.38 V), followed by the untreated AZ31 (–1.39 V), and the E_{corr} of LI and HCDI-LI treated samples were the lowest ones (–1.44 V, –1.52 V). Moreover, the polarisation curves of the untreated, HCDI and LI treated samples demonstrate similar patterns of cathodic kinetics, indicating that HCDI and LI have a little effect on the cathodic kinetics of AZ31 alloys. The polarisation curves showed that the HCDI-LI treated sample had a much lower cathodic current density in the cathodic region. This means that hydrogen evolution from the surface of HCDI-LI treated sample is less intensive than that from the other samples. A slower cathodic reaction on the surface is one of the reasons for a lower corrosion rate of HCDI-LI treated samples. Following the anodic polarisation curve of untreated AZ31 alloy, a small sign of passivity with increasing current densities at potentials above the E_{corr} can be seen (Fig. 4b, Curve 1). For the HCDI and LI treated surfaces, corrosion current quickly increased with a slight increase in potential in the anodic direction. These results suggest that the localised corrosion occurred and the surface of coatings lost its protective function at the corrosion potential (E_{corr}) or even more negative E values. While for the HCDI-LI treated sample emergence of passivation indicated that a stable oxide film was formed on the surface of the alloy, which had a good corrosion resistance, the anodic current density slowly increased from the corrosion potential (E_{corr}) to approximate –1.44 V. Then the corrosion current density quickly increased from –1.44 to –1.37 V, indicating the occurrence of the localised corrosion. Moreover, the localised corrosion potential (breakdown) on the HCDI-LI

Table 1. **Data of the AZ31 alloy obtained from potentiodynamic curves**

Sample	E_{OCP}/V after 3600 s	E_{corr}/V	i_{corr}/μA cm^{-2}	β_c
Untreated AZ31	–1.50	–1.39	11.4	–212.5
HCDI treated	–1.5	–1.38	11.4	–233
LI treated	–1.48	–1.44	18	–214
HCDI-LI treated	–1.57	–1.52	4	–154

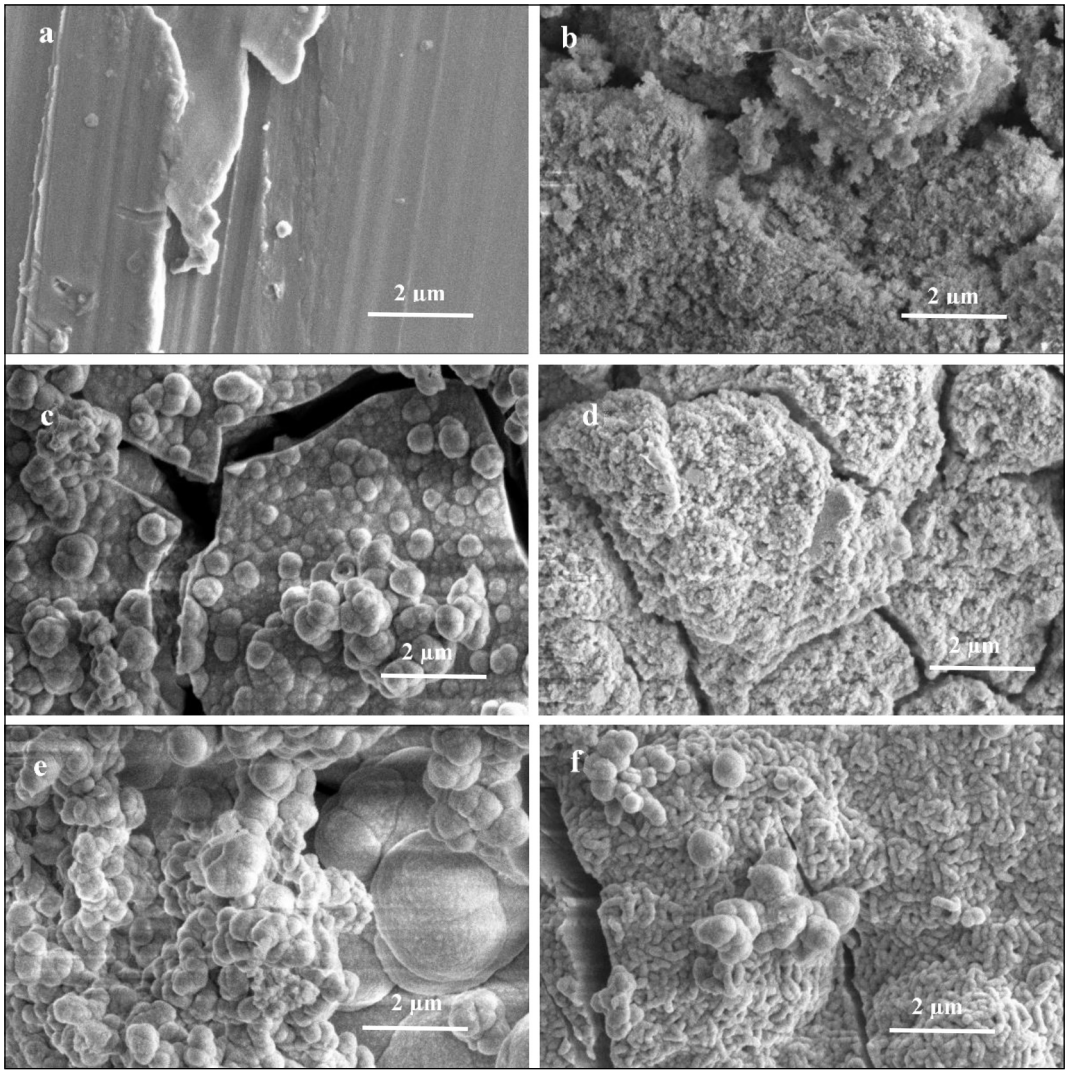

Fig. 5. SEM images of the surfaces of AZ31 alloy after the immersion in Hank's solution (with corrosion products): (a) untreated for 0 h, (b) treated with HCDI-LI for 0 h, (c) untreated for 24 h, (d) treated with HCDI-LI for 24 h, (e) untreated for 72 h and (f) treated with HCDI-LI for 72 h. (a, b, c, d, e, f) lower and higher magnifications

sample was more positive than its corrosion potential, therefore the localised corrosion could not occur spontaneously. The corrosion current density calculated by extrapolating the cathodic region of the Tafel curve of untreated AZ31, the ones treated with HCDI, LI and HCDI-LI are 11.4, 11.4, 18 and 4 μA/cm^2, respectively. These data support the evidence that the HCDI-LI treatment increases the corrosion resistance of AZ31 alloy in Hank's solution.

The SEM images of the surfaces of AZ31 alloy are shown in Fig. 5. The AZ31 alloy after the treatment with HCDI-LI shows a strongly developed surface (Fig. 5b) as compared to that of the untreated AZ31 alloy (Fig. 5a). Such surfaces are reputed to promote biomineralisation and bone biointegration [9].

The long-term corrosion behaviour of untreated and HCDI-LI treated AZ31 alloy samples was investigated by immersion in Hank's solution (Fig. 5c, d, e, f). After 24 h of immersion, the content of Ca and P increased due to the deposition of Ca-containing phosphates from the solution on the surface of the untreated and treated samples (Fig. 5c, d), (Table 2). It should be noted that the cracks in the untreated sample are significantly wider than those in the sample treated with HCDI-LI (Fig. 5c, d). This indicates that a thicker layer of corrosion products is formed on the surface of the untreated specimen, which results in the formation of larger cracks due to internal stresses. This assumption is also confirmed by the data obtained by Tkac et al. [10]. The layer of corrosion products on the HCDI-LI

Table 2. **EDX results after the immersion of AZ31 alloy in Hank's solution**

Sample	Element, at.%					
	Mg	Al	Zn	O	Ca	P
AZ31 untreated	97.46	2.23	0.30	0.00	0.00	0.00
AZ31 treated (HCDI+LI)	58.07	0.91	0.16	40.86	0.00	0.00
AZ31 untreated after immersion for 24 h	42.30	1.23	0.19	46.49	4.53	5.27
AZ31 treated (HCDI+LI) after immersion for 24 h	39.34	1.23	0.11	46.73	6.48	6.10
AZ31 untreated after immersion for 72 h	18.80	0.61	0.05	61.20	10.63	8.71
AZ31 treated (HCDI+LI) after immersion for 72 h	15.12	0.46	0.05	63.13	11.70	9.54

treated surface is significantly more compact (Fig. 5d) as compared to the untreated AZ31 alloy surface (Fig. 5c). This agrees well with the results obtained by Wu et al. [11]. In addition, larger grains of Ca phosphates are formed on the surface of the untreated sample (Fig. 5c). Meanwhile, fine grains are formed on the surface treated with the HCDI-LI method (Fig. 5d). This dependence remains even after 72 h of immersion in Hanks' solution (Fig. 5e, f).

In our case, as shown in Table 2, the Ca/P atomic ratio of untreated AZ31 alloy after 24 h of immersion is 0.86, and the Ca/P atomic ratio of HCDI-LI treated AZ31 is 1.06. Meanwhile, after 72 h of immersion, the Ca/P atomic ratios of treated with HCDI-LI and untreated AZ31 alloy are 1.22 and 1.23, respectively. It should be mentioned that the theoretical Ca/P atomic ratio of hydroxyapatite (HA) is 1.67 [12]. However, both the values after immersion were lower than the theoretical value of HA. Hence, the formed coating was identified to be Ca-deficient HA (CDHA) [13]. Dorozhkin et al. [14] determined that the CDHA in the range of 1.33 to 1.55 for the Ca/P atomic ratio induced the formation of a new bone tissue *in vivo*.

The data obtained in a long-term corrosion study of AZ31 alloy, suggest that the average corrosion rate of untreated AZ31 is approximately 0.55 mg/cm^2/day. Whereas, after AZ31 alloy was treated with HCDI-LI, its average corrosion rate was 0.15 mg/cm^2/day. Such a result is very promising, bearing in mind the fact that the corrosion rate of all Mg alloys *in vivo* is on average about 2.5 times slower than that *in vitro* [15].

CONCLUSIONS

This article presents a new method of AZ31 alloy treatment in order to increase its corrosion resistance. The XRD data obtained reveal that the high current density impulse (HCDI) and laser irradiation (LI) treatment of AZ31 alloy makes it possible to obtain Mg-Al crystallites of the smallest size (16.2 nm) as compared to those of the untreated AZ31 alloy (20.6 nm).

The data of the electrochemical analysis of AZ31 samples suggest that the highest corrosion resistance (i_{corr} = 4.0 μA cm^{-2}) was observed for the AZ31 samples treated with HCDI-LI as compared with that of untreated AZ31 samples (i_{corr} = 11.4 μA cm^{-2}). The treatment of AZ31 alloy by using the HCDI-LI method is an efficient, low-cost and environmentally friendly process that can also be applied for biomaterials. The successive treatment of AZ31 alloy by two methods (HCDI-LI) makes it possible to achieve two goals: to increase the surface area and to enhance the corrosion resistance.

Received 29 April 2022
Accepted 13 May 2022

References

1. F. Witte, N. Hort, C. Vogt, et al., *Curr. Opin. Solid State Mater. Sci*., **12**, 63 (2008).
2. J. Tan, S. Ramakrishna, *Appl. Sci*., **11**, 6861 (2021).
3. Y. Sheng, Y. Hua, X. Wang, et al., *Materials*, **11**, 185 (2018).
4. A. I. Babutsky, A. Chrysanthou, J. Ioannou, *Strength Mater.*, **41(4)**, 387 (2009).
5. A. I. Babutsky, A. Chrysanthou, J. Ioannou, I. Mamuzic, *Mater. Technol.*, **44(2)**, 99 (2010).
6. M.-Z. Ge, J.-Y. Xiang, *J. Alloys Compd.*, **680**, 544 (2016).
7. M.-Zh. Ge, J.-Y. Xiang, L. Yang, J. T. Wang, *Surf. Coat. Technol.*, **310**, 157 (2017).
8. S. Jana, M. Olszta, D. Edwards, et al., *Corr. Sci*., **191**, 109707 (2021).
9. K.-Ch. Chen, T.-M. Lee, N.-W. Kuo, et al., *Mater*., **13**, 1548 (2020).

10. J. Tkacz, K. Slouková, J. Minda, et al., *Metals*, **7**, 465 (2017).
11. C. L. Wu, W. Zai, H. C. Man, *Mater. Today Commun*., **26**, 101922 (2021).
12. S. Ramesh, C. Y. Tan, M. Hamdi, I. Sopyan, W. D. Teng, *Proceedings of International Conference on Smart Materials and Nanotechnology in Engineering*, Harbin (2007).
13. C. Wen, S. Guan, L. Peng, C. Ren, X. Wang, Z. Hu, *Appl. Surf. Sci*., **255**, 6433 (2009).
14. S. V. Dorozhkin, *Prog. Cryst. Growth Charact*., **44(1)**, 45 (2002).
15. M. Esmaily, J. E. Svensson, S. Fajardo, et al., *Prog. Mater. Sci*., **89,** 92 (2017).

Gedvidas Bikulčius, Svetlana Lichušina, Vidas Pakštas, Mindaugas Gedvilas, Voitech Stankevič, Aušra Selskienė, Asta Grigucevičienė

AZ31 LYDINIO, APDOROTO AUKŠTO TANKIO SROVĖS IMPULSU ARBA / IR LAZERIO SPINDULIUOTE, KOROZINIS ATSPARUMAS HANKSO TIRPALE

S a n t r a u k a

Šiame straipsnyje pristatėme naują metodą, kuris gali pagerinti AZ31 lydinio atsparumą korozijai. Palyginome AZ31 lydinio folijos, apdorotos didelio srovės tankio impulsu (HCDI), lazeriu (LI), ir HCDI-LI su neapdorotos folijos biodegradacija. AZ31 lydinio, apdoroto HCDI-LI metodu, biodegradacijos greitis buvo mažesnis nei neapdoroto lydinio, apdoroto HCDI arba LI. Taigi pagerintas AZ31 lydinio, apdoroto HCDI-LI metodu, atsparumas korozijai leidžia jį naudoti medicininiais tikslais.